

327 **Supplemental material**

328 **Video 1** Effects of changing ventilator settings on pulmonary lymphatic valve function and afferent lung  
329 lymph flow

330 **Video 2** Effect of changing ventilator tidal volume on lymph flow within pulmonary lymphatics following  
331 LPS-induced acute lung inflammation

332 **Video 3** Leukocyte dynamics and diversity within pulmonary lymphatics after LPS-induced acute lung  
333 inflammation

334 **Video 4** Effect of pertussis toxin on leukocyte flow within pulmonary lymphatics following LPS-induced  
335 acute lung inflammation

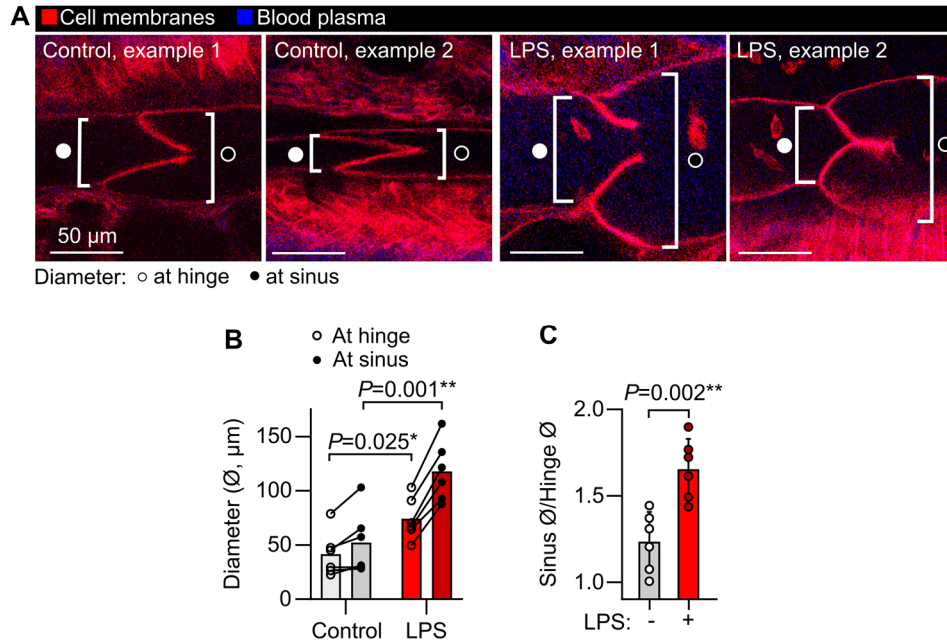
336 **Video 5** Effect of knockout of *Ccr7* on leukocyte flow within pulmonary lymphatics following LPS-  
337 induced acute lung inflammation

338 **Video 6** Effect of *Ccr7* blocking antibody treatment on leukocyte flow within pulmonary lymphatics  
339 following LPS-induced acute lung inflammation

340 **Video 7** Pulmonary lymphatic trafficking of leukocytes, cancer cell material and cancer cells following  
341 lung metastasis of B16.F10 melanoma cells

342 **Supplementary Data File 1** 3D model of thoracic window

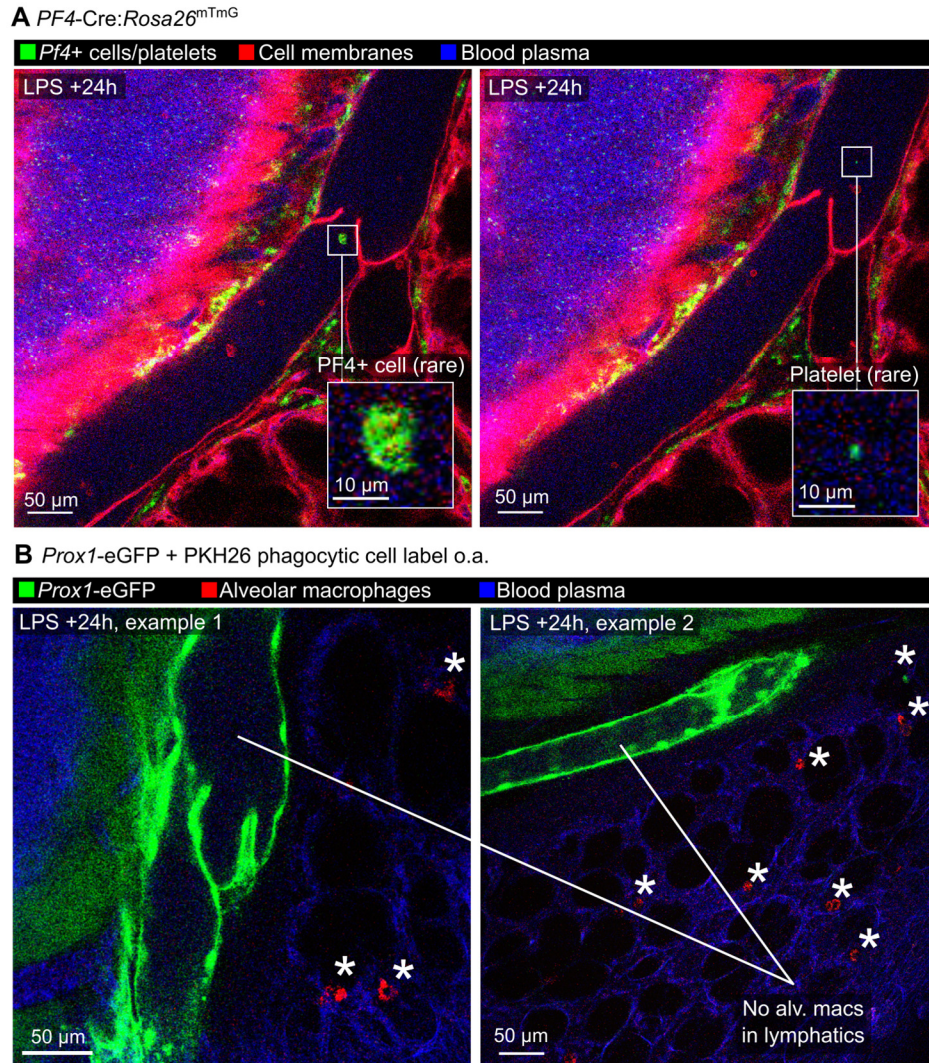
343



631

632 **Figure S1: Measurement of pulmonary lymphatic distension in LPS-induced acute lung inflammation. (A)**  
633 Representative images of pulmonary lymphatic valves from steady state controls and LPS-treated *Rosa26<sup>mTmG</sup>*  
634 mice showing approach for measuring lymphatic diameter. **(B)** Lymphatic vessel diameters at valve hinges and at  
635 sinuses immediately downstream of valves. **(C)** Sinus diameters divided by hinge diameters showing relative  
636 distension of sinuses. Graphs show means  $\pm$  SEM. *P*-values are from: **(B)** repeated measures, 2-way ANOVA  
637 with Holm-Šídák test for effect of LPS within vessel region groups; or **(C)** unpaired, 2-tailed t-test. Group sizes:  
638  $n=6$ .

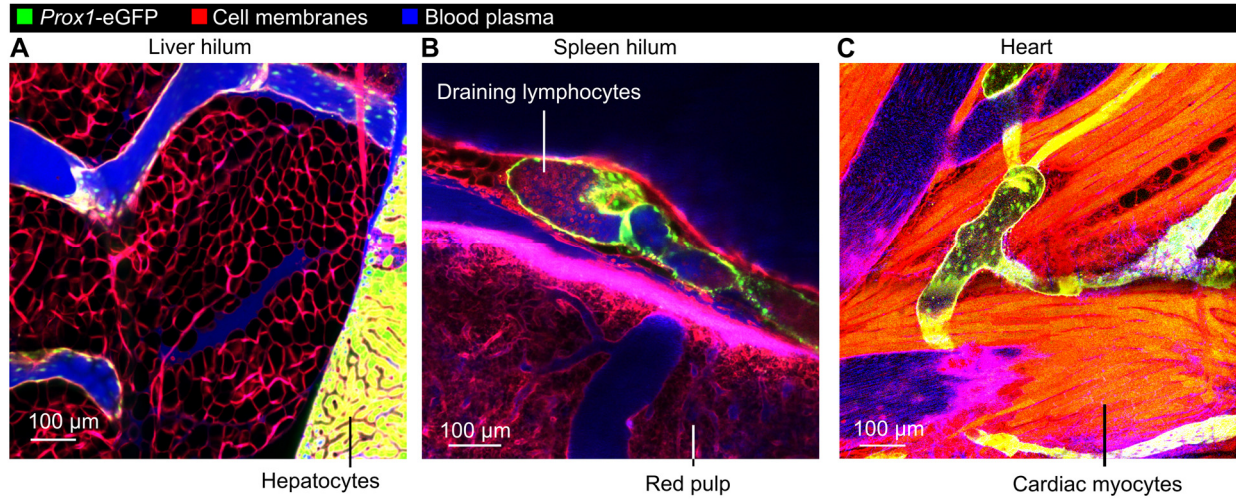
639



640

641 **Figure S2: Imaging of pulmonary lymphatics in LPS-treated *Pf4-Cre:Rosa26<sup>mTmG</sup>* mice and *Prox1-eGFP***  
642 **mice given PKH26-PCL to label alveolar macrophages. (A)** Intravital images of an LPS-treated *Pf4-*  
643 *Cre:Rosa26<sup>mTmG</sup>* mouse showing platelets in blood vessels and recombined cells in bronchovascular cuff spaces  
644 but only very rare recombined cells and possible platelets in lymph. **(B)** *Prox1-eGFP* mice were given an o.a.  
645 dose of PKH26-PCL dye to label alveolar macrophages, then 5 days later mice were given o.a. LPS. Intravital  
646 imaging at 24 hours after LPS treatment showed labeling of alveolar macrophages (alv macs, asterisks) in alveoli  
647 but not in lymphatic vessels.

648



649

650

651

652

653

654

655

656

657

**Figure S3: Stabilized imaging of lymphatic vessels draining the liver, spleen and heart.** *Prox1-eGFP:Rosa26<sup>mTmG</sup>* mice were given Evans blue i.v. prior to stabilized intravital imaging of: (A) the hilum of the liver; (B) the hilum of the spleen; and (C) the ventricular wall of the heart. Note free movement of Evans blue-labeled plasma proteins into liver and spleen draining lymphatics, likely due to the fenestrated endothelium lining blood vessels in these organs, as well as many leukocytes with lymphocyte morphology draining from the spleen, a secondary lymphoid organ.